Coulometric Titration of Active Sites at Mesostructured Cobalt Oxide Spinel by Surface Interrogation Mode of Scanning Electrochemical Microscopy

Julian Lorenz,[a,c,*] *Mingquan Yu,*[b] *Harun Tüysüz,*[b] *Corinna Harms,*[a] *Alexander Dyck,*[a] *Gunther Wittstock*[c,*]

[a] DLR Institute of Networked Energy Systems, Carl-von-Ossietzky-Str. 15, 26129 Oldenburg, Germany

[b] Max-Planck-Institut für Kohlenforschung, Kaiser-Wilhelm-Platz 1, 45470 Mülheim an der Ruhr, Germany

[c] Carl von Ossietzky University of Oldenburg, Chemistry Department, 26111 Oldenburg, Germany

* wittstock@uol.de, +49-441-798-3971

* julian.lorenz@dlr.de, +49-441-99906-323

ABSTRACT

Cobalt-based transition metal oxides are promising candidates for the oxygen evolution reaction. However, a complex interplay between the catalyst crystal structures and material morphologies as well as the surface reactions hampers a comprehensive understanding of the electrocatalytic oxygen evolution reaction at those materials. Here, we investigate the amount and reactivity of specific surface sites of a mesostructured cobalt oxide spinel powder by surface interrogation mode of scanning electrochemical microscopy (SI-SECM). The powder material was supplied in cavity-microelectrodes and efficiently titrated with an Fe(II)-triethanolamine redox mediator generated at a gold microelectrode in alkaline electrolyte. Thus, quantification of different surface sites was achieved and their reactivity showed dependence on the cobalt oxidation state. Titration experiments after adjustable time delays with respect to the generation of the different surface sites indicated that these surface sites are active for the oxygen evolution reaction. Kinetic analysis revealed two pseudo-first order decay constants that were related to fast and slow surface sites for the oxygen evolution reaction. Rate constants were determined for potentials where predominantly a mixed-valence $Co^{III/IV}$ state might be present as most active species. These results expand the great potential of the surface interrogation mode on studying the reaction kinetics of distinct surface sites for practically relevant powdered, non-precious metal catalysts to address a highly relevant challenge in electrocatalysis.

INTRODUCTION

Electrocatalysis of the oxygen reduction reaction (ORR) in fuel cells and the oxygen evolution reaction (OER) in water electrolysis will play a key role in achieving a sustainable energy supply. Both reactions suffer from high overpotentials and complex reaction mechanism including the transfer of four electrons.[1] Metal oxides are discussed as promising alternatives to precious metal catalysts in oxygen electrocatalysis since they are highly abundant and the different oxidation states and their complexing properties can stabilize surface intermediates in the course of catalytic OER and ORR.[2] While various catalyst materials, structures and morphologies are under investigation, a comprehensive understanding of the oxygen electrocatalysis including the correlation between catalyst structure and details of the surface reaction steps has not yet been attained.[1-2] In particular, the identification of catalytically active surface structures, possibly having different structures than the bulk material, requires surface-sensitive *in situ* characterization techniques in connection with reactivity-sensitive methods.[3-6]

The structure-reactivity relationship of metal oxides is frequently addressed by *in situ* or *operando* studies using x-ray absorption spectroscopy (XAS) techniques[3-5, 7-8] and different properties were proposed as activity descriptors for the ORR and OER. Suntivich et al.[9] studied various transition metals by varying systematically the metal cation in the B site of the perovskite structure (ABO_3). They demonstrated that the ORR activity primarily correlates to the occupation of the e_g orbital of the transition metal on the B site, which goes along with its oxidation state. Thus, the transition metal-oxygen covalence can be optimized, which is important for the bonding strength of reaction intermediates.[9] A similar principle was also reported for wide range of spinel oxides ($A^{tetr}B_2{}^{oct}O_4$) where in the normal spinel phase oxygen (or another anion) forms a face-centered cubic structure and the metal ion A (Co^{II}) occupies 1/8

of the tetrahedral sites while the metal ion B (Co^{III}) occupies 1/2 of the octahedral sites (Scheme 1b).[10] The oxidation state of the B cation in the octahedral site was depicted as activity descriptor for oxygen electrocatalysis while the cation in the tetrahedral position seemed to have a minor impact.[7] Furthermore, the bulk formation energy[11] and the number of d electrons[12] of the transition metal or the position of the oxygen p-band center[13] were described as properties determining the activity of OER electrocatalysis.

Recently, a reversible near-surface amorphization of crystalline Co_3O_4 was reported together with the identification of a catalytically active structural motif during the OER.[4, 14] The authors concluded that the onset of the electrocatalytic OER occurs with the oxidation of crystalline Co_3O_4 to an amorphous sub-nanometer shell of $CoO_x(OH)_y$, where di-μ-oxo bridged $Co^{III/IV}$ ions in an octahedral coordination are the active site.[4] (Also tetrahedral coordinated Co^{II} ions change their coordination to octahedral, probably by moving inside vacant octahedral sites in the reactive zone of the amorphous layer.) Interestingly, the same structural motif was also observed in a subsequent study of cobalt oxide compounds with different crystal structures comprising various Co oxidation states and coordination.[14] This means that the di-μ-oxo bridged Co ions in Co(oxyhydr)oxides can be depicted as unified structural motif of catalytically active OER catalysts.[14] Similar structural motifs as active site for the OER were also identified for amorphous or electrodeposited cobalt oxide.[5, 8]

Here, we use the surface interrogation mode of scanning electrochemical microscopy (SI-SECM) to gain additional reactivity information from surface sites on mesostructured spinel cobalt oxides (Co_3O_4) under distinct substrate potentials. The SI-SECM was introduced by Rodriguez-Lopez et al.[15-16] to study surface oxide formation and adsorption of reaction intermediates. The setup uses sample as substrate microelectrode (ME) and an interrogator ME

of equal size as probe, which are placed collinearly with a mutual distance of a few micrometer (Scheme 1a-1).[15] First, the surface species of interest are formed on the sample surface at a defined potential. Then the sample is disconnected from an external voltage source and keeps at open circuit potential (OCP) avoiding the flow of charge except by interfacial reaction at the sample|solution interface. The interrogator electrode then generates the titrant electrolytically from the added mediator. The titrant reaches the sample uniformly by diffusion, where it can react with the surface sites (Scheme 1a-2). During the surface reaction, the original mediator is regenerated and sensed as an enhanced transient feedback current at the interrogator ME. When all surface sites have reacted with the mediator, the mediator regeneration ceases and the ME current decays to the level determined by hindered diffusion from the solution bulk to the interrogator ME (Scheme 1a-3). The recorded current transients (Scheme 1c) provide information about the amount of the surface sites (via the recorded charge) and the reactivity of the surface sites (by the current level). This enables *in situ* quantification of adsorbates and surface oxides even for low coverages and low amount of sample material, which is not possible for spectroscopic techniques.[17] Since SI-SECM is an electrochemical *in situ* technique, the investigated material is not susceptible to chemical transformation induced by a transfer to ultrahigh vacuum or reduction due to secondary electrons caused by X-rays.[17]

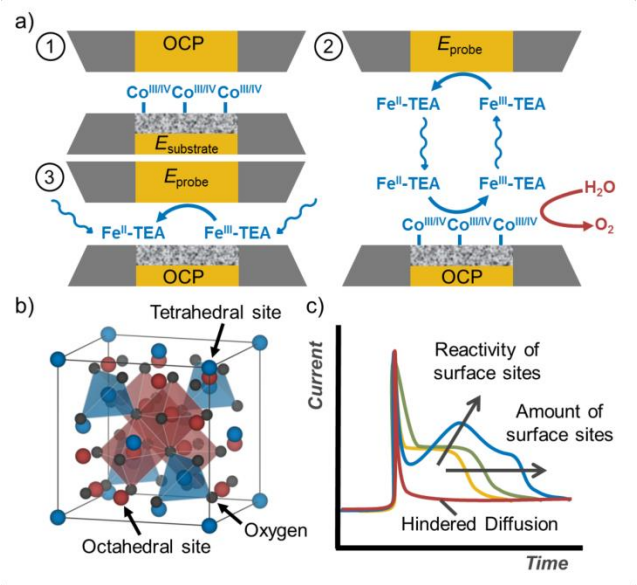

Scheme 1. a) Sequence of the SI-SECM mode with 1) formation of surface sites at the substrate electrode, 2) coulometric titration of surface sites by redox mediator and 3) resulting background current due to hindered diffusion after complete titration (different distances between the electrodes is only for illustration of SI-SECM principle and kept constant in experiments), b) Spinel crystal structure with oxygen in grey, tetrahedral site (metal ion A) in blue and octahedral site (metal ion B) in red, structure was made with the software VESTA[18] and c) Schematic of the obtained current transients of the coulometric titration.

Pioneering work demonstrated the titration of surface oxides on gold and platinum electrodes[15, 19], following that SI-SECM was rapidly expanded to study surface sites and intermediates in oxygen electrocatalysis[17, 20-21] and photoelectrocatalysis.[22-24] Ahn et al.[20] performed time-dependent measurements in a neutral electrolyte and revealed different OER activities for different oxidation states in anodically formed CoP_i material. In another SI-SECM study[17], the coexistence of Ir^{IV} and Ir^{V} oxides during the OER was shown in alkaline solution. For $Ni_{1-x}Fe_xOOH$ ($0 < x < 0.27$), Fe cations were described as fast (more active) sites for the

OER compared to Ni cations based on determined rate constants.[21] These additional possibilities make SI-SECM a valuable *in situ* tool for a detailed analysis of catalytically active sites. Although, SI-SECM cannot identify the chemical structure of active sites, surface-sensitive reactivity studies are achievable for distinct surface sites formed at defined potentials. The SI-SECM experiments discussed above have been limited so far to planar metal oxide films and electrodes. In contrast, almost all technical relevant materials are bulk solids or nanoscale materials with high surface areas. In a previous paper, we have extended the applicability of SI-SECM to noble metal oxides in porous materials such as nanoporous Au or carbon-supported Pt nanoparticles placed in a cavity-microelectrode (CME), for which complete and fast accessibility could be ascertained.[25]

Herein, we use cobalt oxide spinel powders with well-defined mesostructured morphology as the sample in a CME. The ordered mesoporous structure leads to a high specific surface area, which can be employed as a nice model system.[26-28] Cobalt-based materials are widely reported as bifunctional catalyst for both OER and ORR.[29-31] Their activity depends on the oxidation state of near-surface metal cations under applied electrode potential.[4, 7-8] Due to its significant and well separated redox transitions in voltammetry, Co_3O_4 ($Co^{II}Co_2^{III}O_4$) was selected as ideal model compound for SI-SECM, which was studied by the SI-SECM in alkaline solution using the redox couple Fe(III/II) triethanolamine (TEA) ($[Fe^{III/II}(TEA)(OH)]^{-/2-}$). This mediator has been used first by the Bard group[17, 21] for the investigation of other metal oxides in alkaline solution. We varied the potential to track the formation of higher oxidation states on the surface of Co oxides which allowed conclusion about the potential-dependent surface redox states. Furthermore, the kinetics for OER reaction of different surface sites was addressed by the variation of the time between the generation of the surface sites and the onset of the titration

which enabled the reaction of a specific surface site with water during the time delay (red arrow in Scheme 1a-2).

EXPERIMENTAL SECTION

Materials

Hydroxide solutions were prepared using deionized water (18 MΩ cm) and potassium hydroxide powder (Merck, Germany). The redox mediator solution of $[Fe(TEA)(OH)]^-$ was prepared by a procedure described elsewhere.[17, 32] First, 0.25 mmol iron(III) sulfate hydrate ($Fe_2(SO_4)_3 \cdot xH_2O$, Alfa Aesar) were dissolved in 20 mL nitrogen-purged deionized water and stirred for five minutes. To this solution, 0.50 mmol of triethanolamine (Alfa Aesar) was added. Then 20 mL of an ice-cooled 5 M KOH solution was slowly added under stirring. The volume was adjusted to 50 mL upon completion of the synthesis reaction resulting in a 10 mM $[Fe(TEA)(OH)]^-$ solution in 2 M KOH. Mesostructured Co_3O_4 was synthesized as detailed in Supporting Information (SI-1) according to previously published procedure.[26-28]

Instrumentation

Cyclic voltammetry (CVs) and chronoamperometry (CA) were conducted either with an Autolab potentiostat PGSTAT128N under software Nova 2.0 or Nova 2.1 (Metrohm, Germany) or with a Reference 600™ potentiostat (Gamry Instruments Inc., USA). The later instrument was also used for SECM experiments, in which it was controlled by the homemade software SECMx using a homemade hardware abstraction layer and the GamryCom interface.[33] The bipotentiostatic SI-SECM setup was obtained with a second Gamry potentiostat.[34] An

electronically operated switch (DG 412, Maxim Integrated Products, USA) was used to control the time between the generation step at the CME and the detection step at the ME. An Au-ME with 50 µm diameter was used as interrogator electrode. The CME was prepared from Au-ME with the same diameter (see below). A Hg/HgO-electrode was applied as reference electrodes. All potentials are referred to the potential of the reversible hydrogen electrode (RHE, $E_{RHE} \approx E_{Hg/HgO} + 0.099\ V + 0.059\ V \cdot pH$). A coiled platinum wire served as auxiliary electrode. All experiments were conducted in N_2-purged solutions under atmospheric pressure and at room temperature.

Procedures

Cavity-microelectrodes. Au-MEs were prepared from borosilicate glass capillaries (Hilgenberg, Germany) and gold wire (50 mm diameter, Goodfellow, Germany). CMEs were prepared by electrochemical etching of Au-ME under potentiostatic control in 1 M hydrochloric acid solution. The cavity depth was controlled by the etching time and characterized by confocal laser scanning microscopy and scanning electron microscopy. The depth of the particular CME is stated in the nomenclature. For instance, Co_3O_4-$CME_{18\mu m}$ refers to a cavity of 18 µm depth that was filled by Co_3O_4 powder. The CME can easily be filled by tapping into a small amount of Co_3O_4 powder. Reuse of the CME is possible after emptying the cavity in an ultrasonic bath. Details have been provided elsewhere.[25, 28]

SI-SECM. The Au-ME interrogator electrode and the Co_3O_4-filled CME were aligned to a close distance between 2 and 5 µm by a combination of horizontal line scans in the substrate-generation/tip-collection (SG/TC) mode and vertical approach in the feedback mode in 0.1 M

KOH solution. In the SG/TC mode, oxygen is evolved at the Co_3O_4-CME and this oxygen causes a reduction current at the Au-ME. Then the solution was exchanged against the redox mediator solution (10 mM $[Fe(TEA)(OH)]^-$ in 2.0 M KOH). A reproducible starting surface structure was generated by holding the CME potential at 0.74 V for 10 s. Afterwards a defined potential was applied between 0.94 and 1.54 V for 60 s (incremented in intervals of 50 mV for each run) aiming for oxidation of the mixed-valence Co_3O_4 ($Co^{II}Co_2^{III}O_4$) compound to Co^{III} and Co^{IV} surface redox states. Immediately after this step, the CME was set to OCP and coulometric titration was performed at the ME by CA at -0.11 V for 100 to 200 s (depending on the titrated charge). Background transients for the correction of hindered diffusion were obtained by CA experiments at the interrogator electrode without preceding oxidation of the electrocatalysts. Background-corrected ME current transients were integrated to obtain the charge representing the charge of the higher oxidation states of cobalt oxides (relative to Co_3O_4).

Beside the variation of the potential, the time delay τ_d between oxide generation and detection was varied (0.1, 0.2, 0.5, 1.0, 2.0, 5.0, 10.0, and 30.0 s). During τ_d, no reduced form of the redox mediator is available which could reduce the surface sites at the CME. Thus, water oxidation can take place and the surface sites are reduced. The minimum delay $\tau_{d,min}$ (at τ_d = 0 s) was 20 ms as measured with an oscilloscope which is caused by electronically operated switch. This is negligible with respect to the delays at which significant effects were measured ($\tau_{d,min} << \tau_d$) and is neglected for simplicity ($\tau_{d,min} \approx 0$ s). The procedure was performed for three potentials at 1.34, 1.44 and 1.54 V.

RESULTS & DISCUSSION

Cyclic Voltammetry

Co_3O_4, which was synthesized by nanocasting (Figure S1a) using KIT-6-100 as hard template[26-27] and structurally characterized as detailed in the Supporting Information of ref. 28, had a BET surface area of 112 $m^2 g^{-1}$ and the average pore size was 3.8 nm. This high surface area is beneficial for application in heterogeneous catalysis because it provides more catalytically active sites.[29, 35-36] Furthermore, a spinel-type Co_3O_4 with a cubic structure replicated from the hard template was confirmed by X-ray diffraction measurements.[28] Particles of around 8 nm are highly ordered assembled to form the primary domain with the size between 100 and 500 nm (Figure S1b). The nanoparticles display clear lattice fringes with a spacing of 0.24 nm, which can be index to the (311) planes of Co_3O_4 spinel (PDF: 00-042-1467) (Figure 1a). X-ray photoelectron spectroscopy also showed typical spectrum of mixed-valence Co_3O_4 on the sample surface.[28]

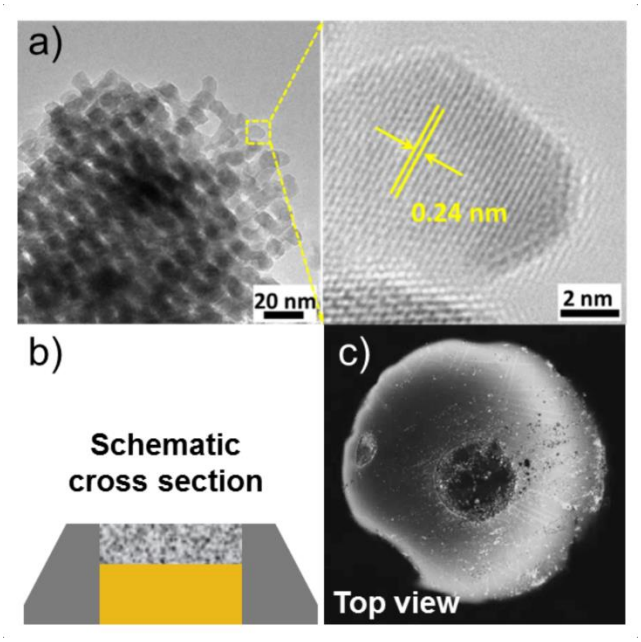

Figure 1. a) High resolution transmission electron microscopy image of the obtained mesostructured Co_3O_4, b) Schematic cross section of the CME and c) top view of a CME filled with Co_3O_4 powder.

Co_3O_4-filled CME (Figure 1b and c) were applied to study the powder material and reproducible voltammograms were obtained in hydroxide solutions with different concentrations (Figure S2a). Cobalt oxides are known to undergo surface amorphization in alkaline electrolytes. Thus, the oxide surface of $Co^{II}Co_2^{III}O_4$ will be partially converted to hydroxides and oxyhydroxides in 2.0 M KOH solution.[37-38] The higher intensity of the redox signals in more concentrated solution originated from the extent of hydroxide/oxyhydroxide formation. Also a slight shift to more negative potentials of the anodic peak was detected which might be a result of a thermodynamically favored oxidation on a more amorphous surface.[37]

A cyclic voltammogram with slower scan rate of ν = 10 mV/s was recorded in order to analyze the amount of less accessible surface sites (Figure 2).[39-40] The voltammogram showed two redox

transitions of Co in the positive-going scan at 1.25 V (I_a) and 1.45 V (II_a). In the negative-going scan, these oxidized sites were reduced (I_c, II_c). The corresponding transitions were described by Trasatti and co-workers[37, 41] as the formation of Co^{III} from Co^{II} and the complete surface oxidation of Co^{III} to Co^{IV} according to Eq. (1) and (2). At more negative potentials, Co^{III} could also be reduced partially to Co^{II} [Eq. (3)] at the surface,[37] but this is not visible at all in our experiments as shown in Figure S2c.

$$Co^{II}Co_2{}^{III}O_4 + H_2O + OH^- \rightarrow 3Co^{III}OOH + e^- \quad (1)$$

$$3Co^{III}OOH + 3OH^- \rightarrow 3Co^{IV}O_2 + 3H_2O + 3e^- \quad (2)$$

$$Co^{II}Co_2{}^{III}O_4 + 2H_2O + 2e^- \rightarrow 3Co^{II}(OH)_2 + 2OH^- \quad (3)$$

For brevity and simplicity, we state the compound in the oxide form as which they were prepared chemically and which forms the bulk of the catalyst powders. The reactions (1)-(3) are used as simplifications, but reaction (3) was not considered in the SI-SECM procedure because it is not visible in our investigation even at lower potential limits in the cyclic voltammogram (Figure S2c). Although the assignments in Eq. (1)-(3) are widely accepted, the extent of the oxidation of Co^{III} to Co^{IV} is a matter of a debate. The identification of Co^{IV} species is very challenging even with spectroscopic techniques.[5, 14, 42-44] In contrast to Eq. (1)-(3), the different redox peaks in the voltammogram have also been described as transition of solely Co^{II} to Co^{III}, where the segmentation results from different structural motifs.[5]

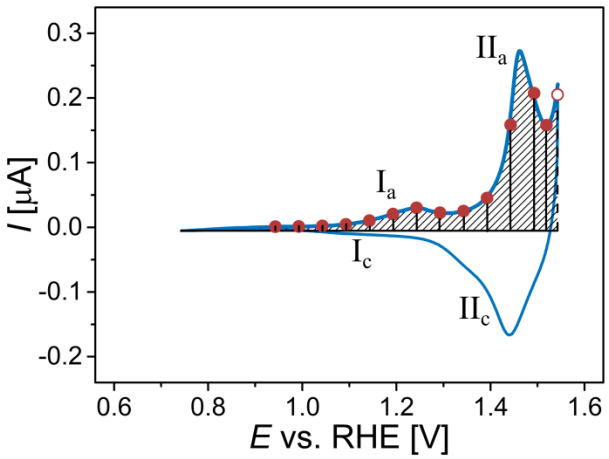

Figure 2. Cyclic voltammograms of Co_3O_4-$CME_{18\mu m}$ at v = 10 mV/s in 2.0 M KOH. The applied SI-SECM potentials are marked as red dots. These potentials were also used as interrogation limits. The redox peaks in the anodic and cathodic scan are labeled I_a and II_a and I_c and II_c, respectively.

Assuming the validity of Eq. (1) and (2), the charge of both oxidation processes should have a ratio of 1:3. We determined a ratio of 1:4.3 in our experiments. The deviation can be explained by irreversible oxidation of possibly present $Co^{II}(OH)_2$ species due to occurring surface amorphization.[45-46] Comparing the 1st and 2nd scan of a cyclic voltammogram in hydroxide solution, a decrease in the current of the peak I_a was observed that is related to the $Co^{II/III}$ transition (Figure S2b). Moreover, not all redox centers that undergo the $Co^{III/IV}$ transition might be active for $Co^{II/III}$ transition.[14] The charge of marked potential intervals in the voltammogram (Figure 2) are used below for comparison to the coulometric titration by SI-SECM.

Potential-Dependent SI-SECM Experiments

After precise collinear alignment of the Co_3O_4-filled CME and the Au-ME interrogator electrode (Figure S3), the electrolyte was exchanged to 10 mM $[Fe(TEA)(OH)]^-$ as redox mediator in 2 M KOH media. The choice of the mediator depends on several properties like the stability under the experimental conditions and the potential difference with respect to the redox couple at the substrate.[16] Redox mediators that are stable under strongly alkaline conditions are very limited and thus $[Fe(TEA)(OH)]^-$ as a robust redox mediator was used.[17, 21]

Coulometric titration was performed at substrate potentials covering the redox peaks I_a and II_a in Figure 2 that are considered for the $Co^{II/III}$ and $Co^{III/IV}$ transitions of cobalt oxides, i.e. from 0.94 to 1.54 V in 50 mV steps (cf. red dots in Figure 2). The reduced form of the mediator $[Fe(TEA)(OH)]^{2-}$ that is generated at the interrogator electrode, reduces the oxidized Co surface sites and is oxidized at the same time (Scheme 1a). The transient positive feedback current sensed at the ME due to this titration process allows for the evaluation of the amount and reactivity of surface sites. However, the SI-SECM method cannot provide structural information or direct determination of oxidation states. Therefore, we relate the measured charges to the literature data summarized above.

CA was used to generate the reduced form of $[Fe(TEA)(OH)]^-$ which underwent a chemical reaction with the cobalt surface sites. The potential to produce the reduced form of the redox mediator was beforehand determined by CV (Figure S4). As already discussed in our pervious study,[25] CA operation at the ME was preferred for coulometric titration experiments over CV because it enabled the detection for largely varying amounts of surface sites. Furthermore, also short-lived species can be detected since the time delay is kept short, during which water can react with the oxidized surface sites. In this context, incorporation of an electronically operated

switch was highly important for a better control of the time delay and faster switching between generation and detection.[20, 47]

The current transients of the subsequent titration steps are shown in Figure S5a and for brevity only exemplary curves shown in Figure 3 are discussed in detail here. The slope of the current transient is very similar to our previous study where gold and platinum surface oxides at porous CME were titrated using $[Ru(NH_3)_6]Cl_3$ as redox mediator in a phosphate buffer solution (pH 6.5).[25] Due to the electron transfer vertically through the conductive network of the porous CME, the surface titration occurs without a diffusional dispersion. The titration mechanism will be discussed in more detail below.

Curve 1 resembles the background and was recorded at the sample without prior oxidation of $Co^{II}Co_2{}^{III}O_4$ states before the titration. The steep decrease in current (more positive current) is based on double layer charging of the interrogator ME and levels off to the steady-state current of hindered diffusion (~ -7 nA, background current). For increasing substrate potentials more negative ME currents were observed due to the reduction of oxidized Co species by the mediator (compare curves 1-7 in Figure S5a). In the current transients a steady-state current of roughly -30 nA is established (Figure 3, curve 2) before the current drops rapidly to the level of negative feedback. The titration process is attributed to the reduction of possibly beforehand formed Co^{III} with $[Fe(TEA)(OH)]^{2-}$ to Co^{II} in the starting compound Co_3O_4 (Eq. (4)). For the current transient recorded after an applied substrate potential of 1.39 V (Figure 3, curve 3), a more negative current was observed during the first 20 s of the CA before the signal reaches again the current plateau of -30 nA. The higher current might originate from the redox titration of additional present Co^{IV} surface sites which might start to appear at this substrate potential (Eq. (5)).

$$Co^{III} + [Fe^{II}(TEA)(OH)]^{2-} \rightarrow Co^{II} + [Fe^{III}(TEA)(OH)]^{-} \quad (4)$$

$$Co^{IV} + [Fe^{II}(TEA)(OH)]^{2-} \rightarrow Co^{III} + [Fe^{III}(TEA)(OH)]^{-} \quad (5)$$

The reaction of the Co oxide can be described as valence change at the oxide surface, which are represented by Eq. (4) and (5) in a simplified form. In fact, the situation is far more complex, because Co ions are in different oxidation states but also in different coordination environment at an oxide surface.

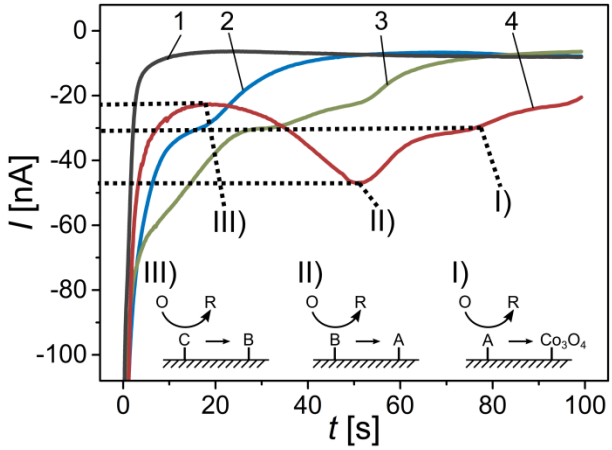

Figure 3. Coulometric titration of surface sites at Co_3O_4-$CME_{18\mu m}$ polarized at specific potentials 1) negative feedback, 2) 1.24 V, 3) 1.39 V and 4) 1.54 V. A set of all record current transients is shown in Figure S5a. Inset shows the anticipated titration of I) state A to Co_3O_4 , II) state B to A and III) state C to B. For explanation of surface states A-C we refer to Table 1.

The current transient of the most positive substrate potential at 1.54 V possess a different shape (Figure 3, curve 4). At this potential a higher amount of Co^{IV} could be present initially and OER might be catalyzed by the emergence of mixed-valence $Co^{III/IV}$ state as active site.[5, 14] The current transient shows three different current levels at the interrogator electrode (labeled as I to III) which reflects different kinetics of the $[Fe(TEA)(OH)]^-$ generation at the Co oxide surface.

First, the current dropped to roughly -20 nA, then increased again to -45 nA and decreases then to -30 nA, a similar level as observed for the other current transients. The current is maintained until all surface sites were titrated followed by a current decay to the value for hindered diffusion. As exact definition of the present surface structure is challenging by electrochemical approaches alone, we denote the state of the oxide surface as A, B and C. Upon variation of the applied potential before the titration step, we can demonstrate that surface state A is formed at potentials between 0.94 and 1.24 V, surface state B between 1.29 and 1.39 V and surface state C between 1.44 and 1.54 V (Table 1).

Table 1. Assignment of surface states to applied substrate potentials in potential-dependent SI-SECM measurements.

Conditioning potential in SI-SECM, $E_{substrate}$ vs. RHE [V]	Co oxidation state after conditioning	Notation for SI-SECM
0.94 – 1.24	Various amounts of Co^{III}	State A
1.29 – 1.39	Mixed-valence state $Co^{III/IV}$	State B
1.44 – 1.54	Mixed-valence state $Co^{III/IV}$ with higher amount of Co^{IV} than in B	State C

We observe slower kinetics for the reaction of state C with $[Fe(TEA)(OH)]^{2-}$ (process III) than with state B, which might originate from a high amount of Co^{IV} initially present at the surface. Once the amount of Co^{IV} decreases the further reduction of state B is faster (process II), which could be explained by the presence of a mixed-valence compound with higher intrinsic conductivity.[14, 48] Thus, a peak is observed after 50 s with currents of around -45 nA. Process I is attributed to the reduction of state A to the pristine compound Co_3O_4. The reaction rate slows down possibly due to an increasing number of Co^{III} states and the current reached the steady-state current of -30 nA (at about 65 s), a similar level as in the previously discussed transients for

the reduction of Co^{III} to Co^{II} (Figure 3, curve 2 and 3, process I). Finally, the current decays to the value of the hindered diffusion. This sequence of processes is also illustrated in Figure S5b. The higher currents at the beginning of the current transients for the substrate potentials of 1.29, 1.34 and 1.39 V can also be explained by generation of the mixed-valence state B enabling faster titration of the porous cobalt oxide electrode by better conduction of charge inside the material (Figures S5a, curves 8-10).

The assignment of surface states A, B and C to signals in the cyclic voltammogram of Co_3O_4 is not trivial. It is reasonable to assume that surface state A is a result of oxidation of $Co^{II}Co_2^{III}O_4$ in the process I_a in Figure 2. The strong signal II_a in Figure 2 should then cause the formation of surface state C at around 1.44 V although the relative amount may be different due to holding the substrate potential in SI-SECM experiments for 60 s. Interestingly, we can clearly distinguish surface state B from either state A or C by SI-SECM by their faster kinetics and the potential range at which it is generated, but there are no corresponding redox transitions in the relevant range in the cyclic voltammogram in Figure 2. A possible explanation is the existence of a mixed-valence state in surface state B that promotes electronic conductivity and leads to a more rapid titration of the porous Co oxide in the CME (*vide infra*).[3, 48]

Beside different reaction rates for different oxidation states of cobalt, various structural motifs of the cobalt ions might also influence the current transients. As suggested by Smith et al.,[5] the redox peaks in the cyclic voltammogram might originate solely from $Co^{II/III}$ transitions and their separation is a consequence of different structural motifs at the surface. Thus, Co surface sites that are only oxidized at higher potential (or are hardly accessible), might possess also a lower reaction rate with the redox mediator during the titration process.

Ahn et al.[20] studied $Co^{II/III}$ and $Co^{III/IV}$ transitions of CoP_i OER catalyst deposited on a planar Au-ME with SI-SECM in neutral electrolyte. The CA experiments showed no influence of various surface sites. In SI-SECM procedure using a porous, powder-filled CME as substrate electrode, the CME exposes an outer surface (with similar accessibility as a planar electrode) and an internal surface which is much larger (Scheme 2). Its accessibility is determined by the nature of the pores. In our example, the pores between the primary particles penetrate the whole material and reach the bottom of the CME. In addition, the primary particles are porous themselves due to the hard-template synthesis. Previously, we had proposed a titration mechanism for the redox titration of gold and platinum surface oxides based on a vertical feedback, where the electron transfer takes place through the electronically conductive network instead of a mechanism based on the slow diffusion of the redox mediator inside the porous electrode.[25] Slow internal diffusion would cause a diffusion tail which was not observed in our pervious experiments with various cavity depths and loadings (Scheme 2a). Furthermore, the hypothesis of a vertical feedback was supported by digital simulation of the titration process.[25] We expect a similar vertical feedback in case of Co_3O_4-filled CME (Scheme 2b). In contrast to nanoporous gold, the electronic conductivity of the cobalt oxide material depends on the electronic properties of the material that change with the redox state. Please note that no conductive carbon material was mixed with Co_3O_4 as it is often done with macroscopic porous transition metal oxide electrodes. The electronic conductivity of cobalt oxide is higher if mixed-valence states or oxygen vacancies in the crystal lattice are present.[3, 48] Consequently, we observe different kinetics of the reaction with the mediator depending on the oxidation states of the cobalt spinel.

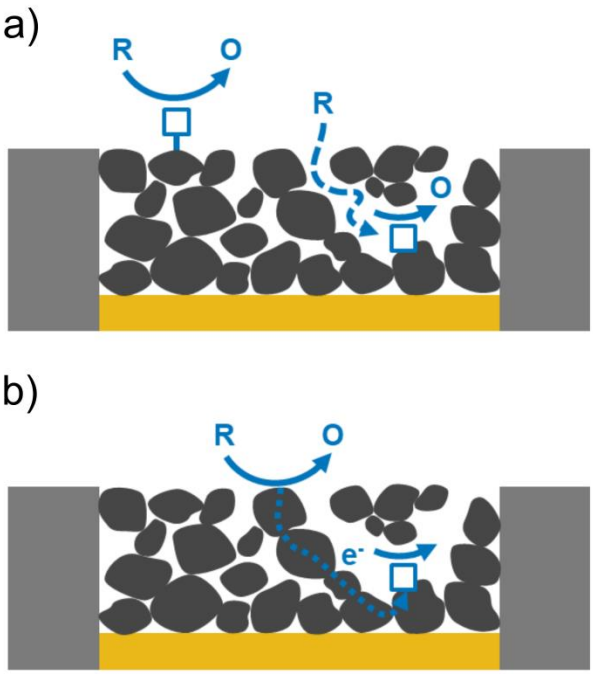

Scheme 2. Proposed titration mechanism of the cavity volume by a) pore diffusion of the mediator and b) a vertical feedback in contrast to the titration of the outer surface. Both represent limiting cases. R corresponds to $[Fe^{II}(TEA)(OH)]^{2-}$, O to $[Fe^{III}(TEA)(OH)]^{-}$ and open squares to surface states (A, B or C).

Similar reactivity-dependent coulometric titration experiments have been described for platinum oxide.[19, 25] There, the reaction of the redox mediator was dependent on the amount of formed oxide layers because Pt and O atoms undergo place exchange for coverages higher than 0.5 monolayers.[49] This goes along with poorer accessibility and decreasing reaction rate. Digital simulation of SI-SECM experiments for Pt/C-filled CME assuming two different rate constants and alternating sequences showed qualitatively a "peak-shaped" current transient if the titration is first dominated by the slower rate constant.[25]

Quantification of the formed surface sites was achieved by integration of current transients and comparison to the transferred charge in cyclic voltammograms. The same Co_3O_4-$CME_{18\mu m}$ electrode but with a fresh filling was used for independent experiments. Figure 4 shows the obtained charges as a function of the applied substrate potentials. The values were reproducibly determined and uncertainties arise from the filling level of the CME and the alignment of the CME and interrogator electrode. The charge in SI-SECM experiments increases continuously to a value of 0.35 µC at a substrate potential of 1.19 V. This charge is related to process I which is most likely described by the reduction of surface state A to Co_3O_4 (Co^{III} to Co^{II}). Then the slope of the Q vs. $E_{substrate}$ plot increases which might indicate a higher rate of Co^{III} formation and the onset of further oxidation to Co^{IV} in the mixed-valence state B. Eventually, a charge of 2.81 µC is transferred for the highest substrate potential of 1.54 V. This charge represents a slight underestimation because the coulometric titration could not be fully completed after 100 s (c.f. Figure 3, curve 4). The transferred charge of the cyclic voltammogram showed a similar trend but with smaller charges for potentials below 1.45 V. This might be due to influence of the scan rate and the lower sensitivity of the voltammetric technique especially at low coverages.[17] The active species is detected in voltammetry by scanning the potential which might already change the interfacial concentration of the species itself leading to a divergence in the analysis of potential-dependent surface coverages. In contrast, the formation and detection in SI-SECM takes place at two different electrodes and is decoupled from each other by setting the substrate electrode to OCP during the titration step.[15-16] At potentials above 1.45 V, a higher charge was obtained by CV possibly due to inclusion of the charge for the incipient oxygen evolution reaction.

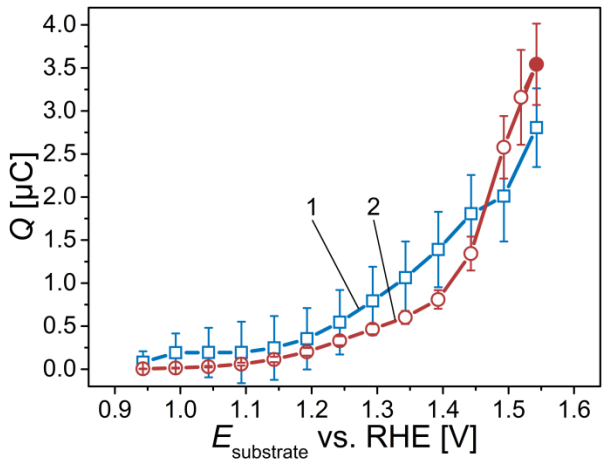

Figure 4. Plot of titrated charge vs. applied substrate potential in SI-SECM (1, blue squares) and in the cyclic voltammograms with integration boundaries in Figure 2 (2, red circles). The red solid circle is influenced by water oxidation. Average of the charge values and their standard deviation are the result of three independent SI-SECM and CV measurements.

Analysis of titrated charge for the current transient after application of 1.54 V to the substrate supports our hypothesis of changing reaction rates for various oxidation states as proposed above (illustrated in Figure S5b). The titration of surface state C and B resulted in a charge of 1.90 µC after 65 s, while the titration from 65 to 100 s gave a charge of 0.64 µC which resembles the reduction of state A. The charge ratio of 3:1 matches the expectation from Eq. (1) and (2) for the stepwise reduction of surface state C to $Co^{II}Co_2^{III}O_4$.

The clear separation of the $Co^{II/III}$ and $Co^{III/IV}$ transitions and the relation to surface states A, B and C (*vide supra*) is difficult both from SI-SECM and CV. The Q vs. $E_{substrate}$ plot from SI-SECM would suggest 1.19 V for the separation of the two transitions (Figure 4). In the current transients of Figure 3, the formation of the mixed-valence $Co^{III/IV}$ state in either state B or C is dominant at 1.39 V, clearly visible at 1.29 V, but may well contribute already at 1.19 V.

Considering the cyclic voltammogram in Figure 2, a more plausible assignment is the formation of mixed-valence $Co^{III/IV}$ at potentials positive of 1.39 V.[14, 37] For the CoP_i catalyst at neutral pH, the two redox processes were separated by application of two different redox mediators.[20] Ferrocenedimethanol was used to reduce a site denoted as "Co^{IV}" completely to the original Co^{II} oxidation state of the starting compound. The Q vs. $E_{substrate}$ plot in Ref. 20 showed a similar trend as in Figure 4 of this work. The second mediator, $IrCl_6^{3-/2-}$ possesses a higher standard potential and was able to reduce selectively Co^{IV} to Co^{III}.[20] By subtracting the charge of the latter process from the charge titrated with ferrocenedimethanol, a differentiation was possible. However, ferrocenedimethanol and $IrCl_6^{3-/2-}$ cannot be used in an alkaline electrolytes that are interesting for OER reaction at transition metal oxides.

SI-SECM is a surface technique, in which surface sites contribute to the signal that are accessible for the electrolyte. This allowed the determination of the surface cobalt atom density by conversion of the titrated charge of the $Co^{II/III}$ process (Supporting Information SI-6).[20-21] In order to estimate the density of affected surface sites, the following were assumed: transfer of one electron for oxidation of $Co^{II}Co_2^{III}O_4$ to 3 $Co^{III}OOH$ and transfer of three electrons for the oxidation of 3 $Co^{III}OOH$ to 3 $Co^{IV}O_2$ and *vice versa*, compare Eq. (1) and (2). These assignments likely represent coarse simplification for the sole purpose of a rough estimation. The calculated charge (Table S1) is related to the electrochemical active surface area of 0.010 cm^2 for Co_3O_4-$CME_{18\mu m}$, which was determined by a procedure described in our previous study[28] by measuring the double layer capacitance in the potential range of ± 50 mV of the OCP and usage of a specific capacitance of 40 µF cm^{-2} for metal oxides surfaces in alkaline solution (Figure S6).[50] Since the coulometric titration of Co^{III} (state A) is a one-electron process, the number of electrons transferred can be directly converted to the amount of accessible Co atoms (but not all

atoms of the formula unit are involved).[20] The titration after applying a substrate potential of 1.54 V resembles the transition of Co^{IV} to Co^{II} and four electrons have to be considered. Calculation of the surface cobalt atom density resulted in values of 12-20 and 12 Co atoms per nm^2 for substrate potentials of 1.19-1.29 V and 1.54 V, respectively. These values are similar to the data from the SI-SECM study of CoP_i where a value of 11 Co atoms per nm^2 was reported[20] and close to other estimations for CoP_i (3 atoms per nm^2) and Co_3O_4 (6 atoms per nm^2).[51-52] Much higher values of around 300 atoms per nm^2 were calculated for nickel-iron mixed oxyhydroxides which was explained by participation of bulk material in the charge transfer.[21]

Time-Dependent SI-SECM Experiments

The introduction of time-dependent SI-SECM experiments enables addressing further research questions in electrocatalysis.[6, 20-21, 24] Thus, not only the amount of surface redox states but also their reactivity towards solution components can be studied yielding the kinetics of distinct surface sites for specific reactions. This was demonstrated on CoP_i in neutral aqueous solution as well as nickel-iron mixed oxyhydroxides in alkaline electrolyte for the OER.[20-21] A time delay τ_d between generation and detection was introduced where in the absence of the reduced form of the redox mediator the electrogenerated surface sites can only react with water. After τ_d, the residual surface sites were quantified by coulometric titration (Scheme 3). Thus, lower titrated charge than in experiments with $\tau_d = 0$ are expected if the surface sites are active for the water oxidation. Variation of the τ_d enables the evaluation of rate laws for distinct surface sites that are adjusted by the substrate potential during the generation step.[20-21, 47]

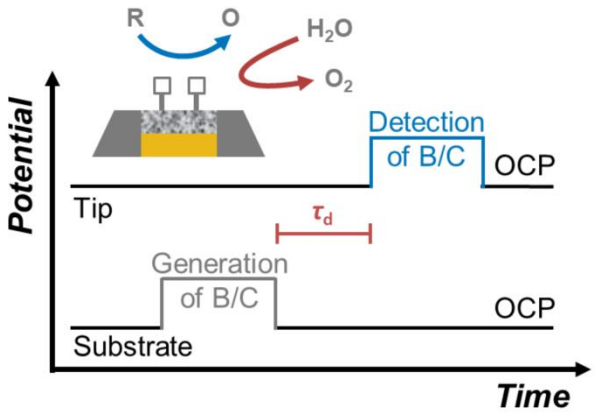

Scheme 3. Potential sequence of time-dependent SI-SECM experiments and respective competitive reactions taking place. R corresponds to $[Fe^{II}(TEA)(OH)]^{2-}$, O to $[Fe^{III}(TEA)(OH)]^{-}$ and open squares to surface states (B or C). The color code of the potential sequence illustrates the generation of surface sites (grey), the reaction of surface sites with water during the time delay (red) and the detection of residual surface sites by the reaction with the redox mediator (blue).

Here, time-dependent SI-SECM experiments were performed for three different substrate potentials 1.34, 1.44 and 1.54 V to form various surface sites and to investigate their OER activity. At 1.34 V mainly the mixed-valence surface state B is formed. At 1.44 and 1.54 V $Co^{III/IV}$ states are formed with different content of Co^{IV} (state C). The applied potential of 1.54 V might lead to a higher amount of Co^{IV} compared to 1.44 V. Current transients and plots of the titrated charge Q vs. τ_d are given in Figure 5. The shape of the current transient remained unchanged with increasing τ_d despite small exceptions. Differences in the current transient and the current level of hindered diffusion originated from independent measurements and thus small differences in the catalyst loading and the alignment. All curves in Figure 5a, except curve 8, exhibited a shoulder at $t \approx 10$ s with a current of ≈ -50 nA. The absence of this shoulder might be

caused by a preferential reaction of water with exactly this Co surface site. The same trend is also evident for the surface sites generated at 1.44 V (Figure 5b). However, a random shift in the peak position of the current transients was observed for the highest substrate potential of 1.54 V (Figure 5c).

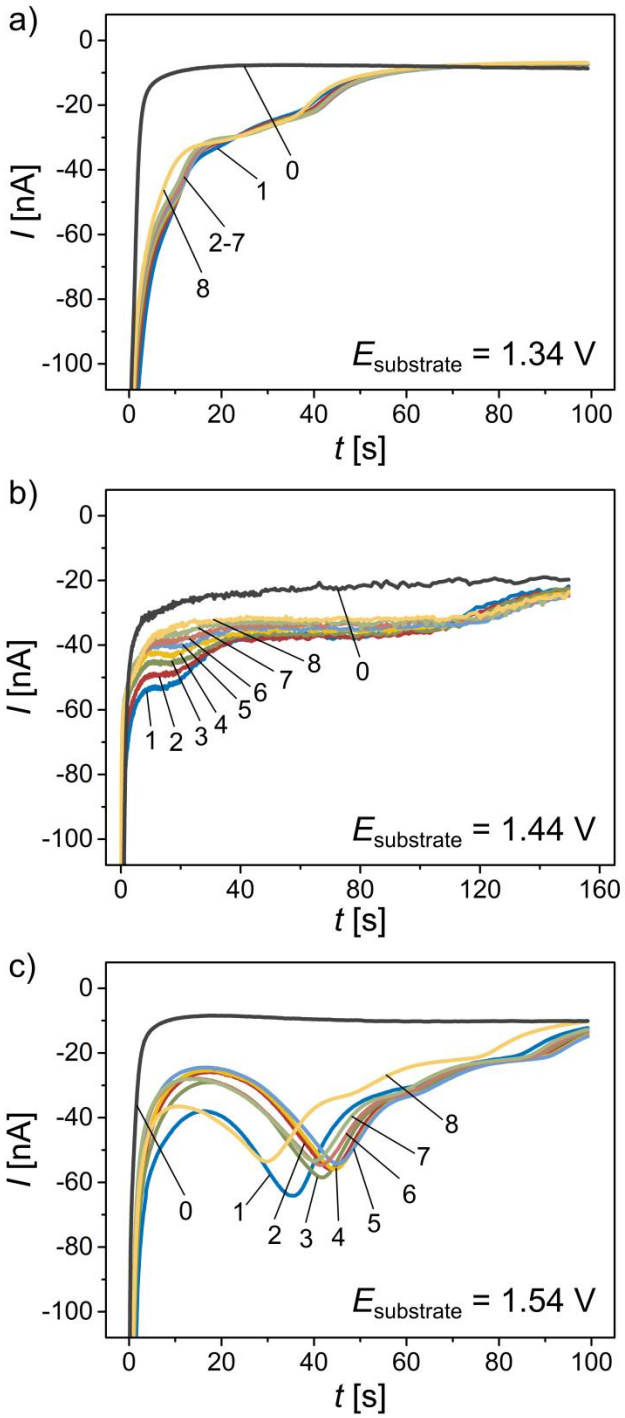

Figure 5. Time-dependent coulometric titration of surface sites by variation of τ_d in the SI-SECM procedure with Co_3O_4-$CME_{18\mu m}$. Current transients 0) background, 1) 0.1 s, 2) 0.2 s, 3) 0.5 s, 4) 1.0 s, 5) 2.0 s, 6) 5.0 s, 7) 10 s and 8) 30 s) for substrate potentials of a) 1.34 V, b) 1.44 V and c) 1.54 V.

During τ_d, oxygen could be produced by water oxidation at the formed surface sites (Scheme S1). Because the Au-interrogator electrode is also catalyzing the oxygen reduction under the applied titration potential, an additional charge might have been detected. Ahn et al.[20-21] expected the formation of $OH^{\bullet}_{ads}$ as the initial step of the OER at the substrate. However, these authors decided not to correct for the effect of possible O_2 or H_2O_2 evolution. We evaluated this influence by background measurements without addition of a redox mediator for the substrate potential of 1.44 V, where a mixed-valence state might be present (Supporting Information SI-7). The detected charge (Figure S7b) emphasizes that oxygen was produced. However, these measurements were not entirely reproducible in our hands as shown by a comparison of curves 1 to 3 in Figure S7b. The amount given in Figure S7b, curve 1 can be seen as upper limit, which represents 30% of the charge extracted by titration with $[Fe(TEA)(OH)]^-$ in Figure 5b. In many cases, the charge for OER made up a much lower percentage of the charge in the titration experiment. Consequently, more Co sites might have reacted in the titration experiments with the redox mediator and the determined rate constants are rather underestimated than overestimated. This possible effect was not directly corrected here, as the quantification of this effect for individual titration experiments is difficult due to requirement of filling and aligning an independent CME.

Nevertheless, lower residual charge values were detected with increasing τ_d for all three substrate potentials (Figure 6a). In all cases, the charge dropped rapidly during the first second. However, the extent of the drop varied from 0.08, 0.33 and 0.45 μC for the potentials of 1.34, 1.44 and 1.54 V, respectively. This indicates formation of sites with higher activity or a larger number of sites for the OER at higher substrate potential. For τ_d between 2 to 30 s the charge decreased more slowly, possibly because most active (or accessible) sites have reacted already.

Differentiation between activity and accessibility and time constants of the SI-SECM process is hardly possible in case of the catalyst volume under investigation in CME. However, our previous study showed a uniform accessibility of cavities with different depths and a fast titration process based on the vertical feedback mechanism.[25] Therefore, we expect that the different slopes originate from surface sites in the Co_3O_4 lattice with different reactivity.

Bergmann et al.[4, 14] identified $CoO_x(OH)_y$ containing di-μ-oxo bridged $Co^{III/IV}$ ions as unified structural motif by application of *in situ* and *operando* surface-sensitive X-ray absorption spectroscopy. This motif was independent of the initial metal valence and coordination in the catalyst material. These authors also evaluated the Co^{III}-reducibility from voltammetry to distinguish fast sites (near-surface Co^{III}-O) and slow sites (non-reducible Co^{III}-O) for the OER.[14] These structurally different active sites could be the basis for the different behaviors in τ_d-dependent titration experiments in this study.

Iron (intentionally added or existed as contamination in the electrolyte) is known to have a beneficial effect on the OER activity of cobalt oxides.[3, 5, 43] The possible influence of contamination by Fe ions from decomposed redox mediator or impurities of the hydroxide solution has to be considered as an alternative explanation for different reaction rates. Smith et al.[5] identified two independent reaction sites on cobalt-iron oxides that catalyze the OER with distinct reaction rates. These different sites might also be responsible for the observation of distinct reaction rates in our study. The sites are a result of the formation of mixed iron-cobalt (oxy)hydroxides. As studied by some of us, the rigid structure of Co_3O_4 obtained by nanocasting was less susceptible to iron contamination[43, 53] than the less crystalline material studied by Smith et al.[5] Cyclic voltammograms recorded after SI-SECM experiments showed that the redox peak I_a at ~1.25 V is vanishing (Figure S8). This could be explained by an anodic shift due to

electronic effects by the substitution of Co^{II} by Fe^{III} or by an irreversible oxidation of some Co^{II} sites to Co^{III} during SI-SECM.[3, 45] Electrochemical impedance spectroscopy showed only a minor effect of the presence of iron in the solution (Figure S9-S11). Further structural analysis of the Co_3O_4 powder is very challenging due to the limited amount of material (~ng range) loaded in the cavity.

For a kinetic analysis the residual charges obtained at different substrate potentials and different time delays (summarized in Figure 6a) were analyzed by modeling two first order decay processes (Supporting Information SI-9). Because no exact statement about the valency of the sites is possible, we used directly the charge. The two pseudo-first order decay constants k_1 and k_2 and corresponding initial charges $Q_1°$ and $Q_2°$ were adjusted for each transient. The obtained values were related to the OER at the fast and slow surface sites (Scheme S2). A fast reaction is evident for the time delay $\tau_d \leq 1$ s. A slow decay is evident for for 2 s $\leq \tau_d \leq$ 30 s from Figure 6a. The statistics of the fitting model yield plausible results summarized in Table S2.

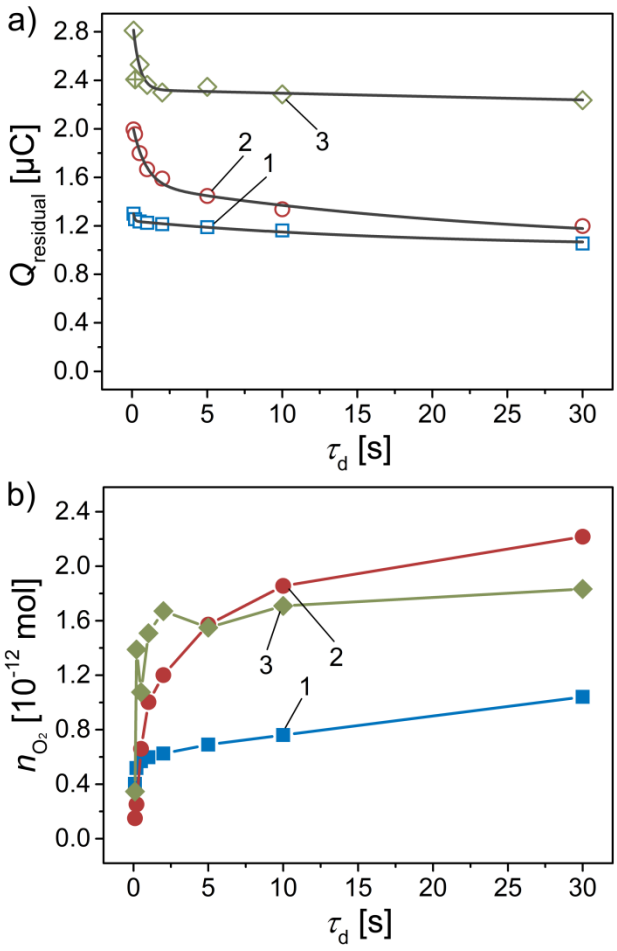

Figure 6. Kinetic analysis of time-dependent SI-SECM experiments for the substrate potentials of 1) 1.34 V (blue squares), 2) 1.44 V (red circles) and 3) 1.54 V (green diamonds). a) Titrated charge of residual surface sites after the time delay and evaluation of two rate constants by the fitting approach described in Supporting Information SI-9. In curve 3, the outlier at a τ_d = 0.2 s (open diamond with cross) was not included in the fit. The results and statistics of the fit are detailed in Table S2. b) Evaluation of the equivalent amount of evolved O_2 (n = 4) during τ_d. Lines in a) are the fit and lines in b) are guides to the eye.

The decay of the charge in τ_d-dependent SI-SECM experiments for all substrate potentials indicates that the formed surface sites are active for the OER. However, the prolonged catalysis

does not take place at the potential of 1.34 V where surface state B is present. As discussed above we denote this state to be likely $Co^{III/IV}$ with a high content of Co^{III}. These Co^{III} species are often not considered as active site for the OER.[20] This assignment might originate from the slow charge-transfer rate constants between Co^{II} and Co^{III}.[54] Thus, water oxidation stops when bulk Co^{III} states are isolated from solution due to formed Co^{II} species at the surface after the first reduction of Co^{III}.[20] Nevertheless, Co^{III} was also described in other studies as active for the OER.[14, 20] Here, rate constants of 12.489 and 0.056 s^{-1} were determined for the situation at a substrate potential of 1.34 V, which are substantial higher than the previously reported value for CoP_i (0.19 s^{-1}) from time-dependent experiments.[20] While the valency of the surface site cannot be determined by SI-SECM, the relation of residual charge to the amount of O_2 formed is given by $4OH^- \rightarrow O_2 + 2H_2O + 4e^-$. Converting the difference for the charge at $\tau_d = 0$ s and $\tau_d = t$ [Eq. (S11)] yields the amount n_{O_2} of O_2 formed (Figure 6b). For all generation potentials there is an initial fast O_2 formation rate, which levels off. Especially curve 3 shows a slower rate for $\tau_d > 2$ s compared to curve 1 and 2.

At a potential of 1.44 V, the possibly present mixed-valence state $Co^{III/IV}$ possesses rate constants of 1.167 and 0.041 s^{-1} for fast and slow decays that are comparable to the values of 2.337 and 0.002 s^{-1} at a potential of 1.54 V. These values are hardly transferrable in an OER activity, but the presence of fast and slow sites is evident from the kinetic analysis. In case of O_2 equivalents, slightly higher values were observed for a substrate potential of 1.44 V compared to 1.54 V (Figure 6b). This indicates that a higher amount of Co^{IV}, which could be present at 1.54 V, might not be beneficial for the OER which is in agreement with the findings in other studies.[55-56] In contrast, Ahn et al.[47] obtained values of 1.2 s^{-1} for the Co^{IV} state of a CoP_i catalyst in neutral solution, which indicates that it might be more active for the OER than the Co^{III} state.[20]

In the study of Bergmann et al.,[14] the less-crystalline CoOOH catalyst was described as more active than Co_3O_4 due to the higher ratio of reducible Co^{III} species. Also, some of us reported recently that amorphous Co-based catalysts show higher OER activity since the active species CoOOH is preferred to form at a less rigid structure.[43] This could be explained by an easier surface reconstruction of the amorphous material.

CONCLUSION

The surface interrogation mode of scanning electrochemical microscopy allows the investigation of electrocatalytic reactions by studying catalytic active surface sites under potential and time control. In contrast to previously studied planar electrodes, the study of catalyst powders by this methodology is enabled by powder-filled cavity-microelectrodes as substrates. The cobalt oxide spinel under investigation was oxidized to form specific surface sites which were efficiently titrated by utilization of iron triethanolamine as redox mediator in highly alkaline electrolyte. The titration mechanism is based on an electron transfer through the conductive network of the catalyst which was proven by careful analysis of the shape of the current transients in dependence on the varied substrate potential. Evaluation of different cobalt oxidation states as a function of the applied substrate potential was achieved by integration of current transients. Moreover, higher reactivity of the mixed-valence cobalt states was demonstrated. The obtained charge is comparable to the charge obtained by cyclic voltammetry of the catalyst powder. However, the surface interrogation mode offers several advantages such as higher sensitivity at low coverages and unaffected detection of oxidation states since the catalyst powder is at open circuit potential. The results were further used to evaluate the amount of surface sites which are potentially available for catalyzing a specific reaction.

Furthermore, time-dependent coulometric titration experiments shed light on the reaction kinetics of the distinct surface sites for the oxygen evolution reaction. During a time delay, the generated cobalt surface sites reacted with water and were subsequently not detectable by surface interrogation. Thus, variation of the time delay allowed a kinetic analysis of specific surface sites and revealed the presence of fast and slow reacting sites in agreement with literature. These distinct sites might be related to different structural motifs of the cobalt. Although the oxidized surface of Co^{III} is usually formed before the onset of oxygen evolution, its catalytic activity was proven. At each of the tested generation potentials two different decay constants were obtained in SI-SECM experiments with variable time delay between the regeneration and titration pulses. Especially the mixed-valence state $Co^{III/IV}$ formed at a substrate potential of 1.44 V resulted in the largest formation of O_2. Thus, our results indicate the dominant role of a mixed-valence cobalt ion in oxygen evolution reaction in accordance with studies using different experimental approaches. These findings emphasize the ability of the surface interrogation mode to study catalytically active sites at technical relevant materials and to evaluate the reactivity of specific surface sites in powdered material. Consequently, this *operando* method approaches the solution of a highly relevant challenge in electrocatalysis.

ASSOCIATED CONTENT

Supporting Information. Nanocasting procedure; Cyclic voltammetry of Co_3O_4, Alignment of microelectrodes; Cyclic voltammetry of $[Fe(TEA)(OH)]^{-/2-}$; Complete data set of potential-dependent SI-SECM; Evaluation of potential-dependent SI-SECM; Background measurements of time-resolved SI-SECM; Evaluation of iron contamination, Evaluation of time-dependent SI-SECM.

AUTHOR INFORMATION

Corresponding Author

Prof. Dr. Gunther Wittstock, Carl von Ossietzky University of Oldenburg, Chemistry Department, 26111 Oldenburg, Germany, wittstock@uol.de, +49-441-798-3971

Julian Lorenz, DLR Institute of Networked Energy Systems, Carl-von-Ossietzky-Str. 15, 26129 Oldenburg, Germany, julian.lorenz@dlr.de, +49-441-99906-323

Author Contributions

The manuscript was written through contributions of all authors. All authors have given approval to the final version of the manuscript.

Funding Sources

Work at the University of Oldenburg (GW, JL) was partially supported by Deutsche Forschungsgemeinschaft (WI1617/20-1) and the University. The work of MY and HT was partially supported by the MAXNET Energy consortium and IMPRS-RECHARGE of Max Planck Society. JL, CH and AD thank for support by the Federal Ministry for Economic Affairs and Energy as basis funding of DLR.

ACKNOWLEDGMENT

The authors acknowledge Gerd Gertjegerdes (University of Oldenburg) for the integration of the electronically operated switch in the SI-SECM set up, Dr. Xiaohui Deng (Max-Planck-Institut

für Kohlenforschung) for help with preparation of cobalt oxide sample, and Eko Budiyanto for taking HR-TEM images. Work at the University of Oldenburg (GW, JL) was partially supported by Deutsche Forschungsgemeinschaft (WI1617/20-1) and the University. The work of MY and HT was partially supported by the MAXNET Energy consortium and IMPRS-RECHARGE of Max Planck Society. JL, CH and AD thank for support by the Federal Ministry for Economic Affairs and Energy as basis funding of DLR.

REFERENCES

1. Katsounaros, I.; Cherevko, S.; Zeradjanin, A. R.; Mayrhofer, K. J. J. Oxygen Electrochemistry as a Cornerstone for Sustainable Energy Conversion. *Angew. Chem. Int. Ed.* **2014,** *53*, 102-121.
2. Hong, W. T.; Risch, M.; Stoerzinger, K. A.; Grimaud, A.; Suntivich, J.; Shao-Horn, Y. Toward the Rational Design of Non-Precious Transition Metal Oxides for Oxygen Electrocatalysis. *Energy Environ. Sci.* **2015,** *8*, 1404-1427.
3. Burke, M. S.; Kast, M. G.; Trotochaud, L.; Smith, A. M.; Boettcher, S. W. Cobalt–Iron (Oxy)hydroxide Oxygen Evolution Electrocatalysts: The Role of Structure and Composition on Activity, Stability, and Mechanism. *J. Am. Chem. Soc.* **2015,** *137*, 3638-3648.
4. Bergmann, A.; Martinez-Moreno, E.; Teschner, D.; Chernev, P.; Gliech, M.; de Araújo, J. F.; Reier, T.; Dau, H.; Strasser, P. Reversible Amorphization and the Catalytically Active State of Crystalline Co_3O_4 during Oxygen Evolution. *Nat. Commun.* **2015,** *6*, 8625.
5. Smith, R. D. L.; Pasquini, C.; Loos, S.; Chernev, P.; Klingan, K.; Kubella, P.; Mohammadi, M. R.; Gonzalez-Flores, D.; Dau, H. Spectroscopic Identification of Active Sites for the Oxygen Evolution Reaction on Iron-Cobalt Oxides. *Nat. Commun.* **2017,** *8*, 2022.
6. Bard, A. J. Inner-Sphere Heterogeneous Electrode Reactions. Electrocatalysis and Photocatalysis: The Challenge. *J. Am. Chem. Soc.* **2010,** *132*, 7559-7567.
7. Wei, C.; Feng, Z.; Scherer, G. G.; Barber, J.; Shao-Horn, Y.; Xu, Z. J. Cations in Octahedral Sites: A Descriptor for Oxygen Electrocatalysis on Transition-Metal Spinels. *Adv. Mater.* **2017,** *29*, 1606800.
8. Risch, M.; Ringleb, F.; Kohlhoff, M.; Bogdanoff, P.; Chernev, P.; Zaharieva, I.; Dau, H. Water Oxidation by Amorphous Cobalt-Based Oxides: *in situ* Tracking of Redox Transitions and Mode of Catalysis. *Energy Environ. Sci.* **2015,** *8*, 661-674.
9. Suntivich, J.; Gasteiger, H. A.; Yabuuchi, N.; Nakanishi, H.; Goodenough, J. B.; Shao-Horn, Y. Design Principles for Oxygen-Reduction Activity on Perovskite Oxide Catalysts for Fuel Cells and Metal–Air Batteries. *Nat. Chem.* **2011,** *3*, 546-550.
10. Zhao, Q.; Yan, Z.; Chen, C.; Chen, J. Spinels: Controlled Preparation, Oxygen Reduction/Evolution Reaction Application, and Beyond. *Chem. Rev.* **2017,** *117*, 10121-10211.
11. Calle-Vallejo, F.; Díaz-Morales, O. A.; Kolb, M. J.; Koper, M. T. M. Why Is Bulk Thermochemistry a Good Descriptor for the Electrocatalytic Activity of Transition Metal Oxides? *ACS Catal.* **2015,** *5*, 869-873.
12. Bockris, J. O. M.; Otagawa, T. The Electrocatalysis of Oxygen Evolution on Perovskites. *J. Electrochem. Soc.* **1984,** *131*, 290-302.
13. Subbaraman, R.; Tripkovic, D.; Chang, K.-C.; Strmcnik, D.; Paulikas, A. P.; Hirunsit, P.; Chan, M.; Greeley, J.; Stamenkovic, V.; Markovic, N. M. Trends in Activity for the Water Electrolyser Reactions on 3d M(Ni,Co,Fe,Mn) Hydr(oxy)oxide Catalysts. *Nat. Mater.* **2012,** *11*, 550.
14. Bergmann, A.; Jones, T. E.; Martinez Moreno, E.; Teschner, D.; Chernev, P.; Gliech, M.; Reier, T.; Dau, H.; Strasser, P. Unified Structural Motifs of the Catalytically Active State of Co(oxyhydr)oxides during the Electrochemical Oxygen Evolution Reaction. *Nat. Catal.* **2018,** *1*, 711-719.

15. Rodríguez-López, J.; Alpuche-Avilés, M. A.; Bard, A. J. Interrogation of Surfaces for the Quantification of Adsorbed Species on Electrodes: Oxygen on Gold and Platinum in Neutral Media. *J. Am. Chem. Soc.* **2008,** *130*, 16985-16995.
16. Rodríguez-López, J. In *Electroanalytical Chemistry: A Series of Advances* Bard, A. J.; Zoski, C. G., Eds. CRC Press Boca Raton, Florida, 2012; Vol. 24, pp 287–352.
17. Arroyo-Currás, N.; Bard, A. J. Iridium Oxidation as Observed by Surface Interrogation Scanning Electrochemical Microscopy. *J. Phys. Chem. C* **2015,** *119*, 8147-8154.
18. Momma, K.; Izumi, F. VESTA 3 for Three-Dimensional Visualization of Crystal, Volumetric and Morphology Data. *J. Appl. Crystallogr.* **2011,** *44*, 1272-1276.
19. Rodriguez-Lopez, J.; Minguzzi, A.; Bard, A. J. Reaction of Various Reductants with Oxide Films on Pt Electrodes As Studied by the Surface Interrogation Mode of Scanning Electrochemical Microscopy (SI-SECM): Possible Validity of a Marcus Relationship. *J. Phys. Chem. C* **2010,** *114*, 18645-18655.
20. Ahn, H. S.; Bard, A. J. Surface Interrogation of CoP_i Water Oxidation Catalyst by Scanning Electrochemical Microscopy. *J. Am. Chem. Soc.* **2015,** *137*, 612-615.
21. Ahn, H. S.; Bard, A. J. Surface Interrogation Scanning Electrochemical Microscopy of $Ni_{1-x}Fe_xOOH$ ($0 < x < 0.27$) Oxygen Evolving Catalyst: Kinetics of the "fast" Iron Sites. *J. Am. Chem. Soc.* **2016,** *138*, 313-318.
22. Zigah, D.; Rodriguez-Lopez J Fau - Bard, A. J.; Bard, A. J. Quantification of Photoelectrogenerated Hydroxyl Radical on TiO_2 by Surface Interrogation Scanning Electrochemical Microscopy. *Phys. Chem. Chem. Phys.* **2012,** *14*, 12764–12772.
23. Simpson, B. H.; Rodríguez-López, J. Electrochemical Imaging and Redox Interrogation of Surface Defects on Operating $SrTiO_3$ Photoelectrodes. *J. Am. Chem. Soc.* **2015,** *137*, 14865-14868.
24. Rastgar, S.; Wittstock, G. In Situ Microtitration of Intermediates of Water Oxidation Reaction at Nanoparticles Assembled at Water/Oil Interfaces. *J. Phys. Chem. C* **2018,** *122*, 12963-12969.
25. Haensch, M.; Behnken, J.; Balboa, L.; Dyck, A.; Wittstock, G. Redox Titration of Gold and Platinum Surface Oxides at Porous Microelectrodes. *Phys. Chem. Chem. Phys.* **2017,** *19*, 22915-22925.
26. Grewe, T.; Deng, X.; Weidenthaler, C.; Schüth, F.; Tüysüz, H. Design of Ordered Mesoporous Composite Materials and Their Electrocatalytic Activities for Water Oxidation. *Chem. Mater.* **2013,** *25*, 4926-4935.
27. Grewe, T.; Deng, X.; Tüysüz, H. Influence of Fe Doping on Structure and Water Oxidation Activity of Nanocast Co_3O_4. *Chem. Mater.* **2014,** *26*, 3162-3168.
28. Behnken, J.; Yu, M.; Deng, X.; Tüysüz, H.; Harms, C.; Dyck, A.; Wittstock, G. Oxygen Reduction Reaction Activity of Mesostructured Cobalt-Based Metal Oxides Studied with the Cavity-Microelectrode Technique. *ChemElectroChem* **2019,** *6*, 3460-3467.
29. Sa, Y. J.; Kwon, K.; Cheon, J. Y.; Kleitz, F.; Joo, S. H. Ordered Mesoporous Co_3O_4 Spinels as Stable, Bifunctional, Noble Metal-Free Oxygen Electrocatalysts. *J. Mater. Chem. A* **2013,** *1*, 9992-10001.
30. Pletcher, D.; Li, X.; Price, S. W. T.; Russell, A. E.; Sönmez, T.; Thompson, S. J. Comparison of the Spinels Co_3O_4 and $NiCo_2O_4$ as Bifunctional Oxygen Catalysts in Alkaline Media. *Electrochim. Acta* **2016,** *188*, 286-293.
31. Menezes, P. W.; Indra, A.; González-Flores, D.; Sahraie, N. R.; Zaharieva, I.; Schwarze, M.; Strasser, P.; Dau, H.; Driess, M. High-Performance Oxygen Redox Catalysis with

Multifunctional Cobalt Oxide Nanochains: Morphology-Dependent Activity. *ACS Catal.* **2015,** *5*, 2017-2027.
32. Arroyo-Currás, N.; Hall, J. W.; Dick, J. E.; Jones, R. A.; Bard, A. J. An Alkaline Flow Battery Based on the Coordination Chemistry of Iron and Cobalt. *J. Electrochem. Soc.* **2015,** *162*, A378-A383.
33. Nunes Kirchner, C.; Hallmeier, K. H.; Szargan, R.; Raschke, T.; Radehaus, C.; Wittstock, G. Evaluation of Thin Film Titanium Nitride Electrodes for Electroanalytical Applications. *Electroanalysis* **2007,** *19*, 1023-1031.
34. *BiPotentiostat Installation and Setup*; Gamry Instruments, Inc.: Warminster, PA, 2017.
35. Tüysüz, H.; Hwang, Y. J.; Khan, S. B.; Asiri, A. M.; Yang, P. Mesoporous Co_3O_4 as an Electrocatalyst for Water Oxidation. *Nano Res.* **2013,** *6*, 47-54.
36. Deng, X.; Schmidt, W. N.; Tüysüz, H. Impacts of Geometry, Symmetry, and Morphology of Nanocast Co_3O_4 on Its Catalytic Activity for Water Oxidation. *Chem. Mater.* **2014,** *26*, 6127-6134.
37. Boggio, R.; Carugati, A.; Trasatti, S. Electrochemical Surface Properties of Cobalt Oxide (Co_3O_4) Electrodes. *J. Appl. Electrochem.* **1987,** *17*, 828-40.
38. Garavaglia, R.; Mari, C. M.; Trasatti, S. Physicochemical Characterization of Co_3O_4 Prepared by Thermal Decomposition II: Response to Solution pH. *Surface Technology* **1984,** *23*, 41-47.
39. Ardizzone, S.; Fregonara, G.; Trasatti, S. "Inner" and "Outer" Active Surface of RuO_2 Electrodes. *Electrochim. Acta* **1990,** *35*, 263-267.
40. Minguzzi, A.; Fan, F.-R. F.; Vertova, A.; Rondinini, S.; Bard, A. J. Dynamic Potential-pH Diagrams Application to Electrocatalysts for Water Oxidation. *Chemical Science* **2012,** *3*, 217-229.
41. Spinolo, G.; Ardizzone, S.; Trasatti, S. Surface Characterization of Co_3O_4 Electrodes Prepared by the Sol-Gel Method. *J. Electroanal. Chem.* **1997,** *423*, 49-57.
42. Favaro, M.; Yang, J.; Nappini, S.; Magnano, E.; Toma, F. M.; Crumlin, E. J.; Yano, J.; Sharp, I. D. Understanding the Oxygen Evolution Reaction Mechanism on CoO_x using Operando Ambient-Pressure X-ray Photoelectron Spectroscopy. *J. Am. Chem. Soc.* **2017,** *139*, 8960-8970.
43. Moon, G.-h.; Yu, M.; Chan, C. K.; Tüysüz, H. Highly Active Cobalt-Based Electrocatalysts with Facile Incorporation of Dopants for the Oxygen Evolution Reaction. *Angew. Chem. Int. Ed.* **2019,** *58*, 3491-3495.
44. Yeo, B. S.; Bell, A. T. Enhanced Activity of Gold-Supported Cobalt Oxide for the Electrochemical Evolution of Oxygen. *J. Am. Chem. Soc.* **2011,** *133*, 5587-5593.
45. Yang, J.; Cooper, J. K.; Toma, F. M.; Walczak, Karl A.; Favaro, M.; Beeman, Jeffrey W.; Hess, Lucas H.; Wang, C.; Zhu, C.; Gul, S.; Yano, J.; Kisielowski, C.; Schwartzberg, A.; Sharp, Ian D. A Multifunctional Biphasic Water Splitting Catalyst Tailored for Integration with High-Performance Semiconductor Photoanodes. *Nat. Mater.* **2017,** *16*, 335-341.
46. Totir, D.; Mo, Y.; Kim, S.; Antonio, M. R.; Scherson, D. A. In Situ Co K‐Edge X‐Ray Absorption Fine Structure of Cobalt Hydroxide Film Electrodes in Alkaline Solutions. *J. Electrochem. Soc.* **2000,** *147*, 4594-4597.
47. Ahn, H. S.; Bard, A. J. Switching Transient Generation in Surface Interrogation Scanning Electrochemical Microscopy and Time-of-Flight Techniques. *Anal. Chem.* **2015,** *87*, 12276-12280.

48. Mizokawa, T.; Wakisaka, Y.; Sudayama, T.; Iwai, C.; Miyoshi, K.; Takeuchi, J.; Wadati, H.; Hawthorn, D. G.; Regier, T. Z.; Sawatzky, G. A. Role of Oxygen Holes in Li_xCoO_2 Revealed by Soft X-Ray Spectroscopy. *Phys. Rev. Lett.* **2013,** *111*, 056404.
49. Jerkiewicz, G.; Vatankhah, G.; Lessard, J.; Soriaga, M. P.; Park, Y.-S. Surface-Oxide Growth at Platinum Electrodes in Aqueous H_2SO_4: Reexamination of its Mechanism Through Combined Cyclic-Voltammetry, Electrochemical Quartz-Crystal Nanobalance, and Auger Electron Spectroscopy Measurements. *Electrochim. Acta* **2004,** *49*, 1451-1459.
50. McCrory, C. C. L.; Jung, S.; Peters, J. C.; Jaramillo, T. F. Benchmarking Heterogeneous Electrocatalysts for the Oxygen Evolution Reaction. *J. Am. Chem. Soc.* **2013,** *135*, 16977-16987.
51. Esswein, A. J.; McMurdo, M. J.; Ross, P. N.; Bell, A. T.; Tilley, T. D. Size-Dependent Activity of Co_3O_4 Nanoparticle Anodes for Alkaline Water Electrolysis. *J. Phys. Chem. C* **2009,** *113*, 15068-15072.
52. Ahn, H. S.; Tilley, T. D. Electrocatalytic Water Oxidation at Neutral pH by a Nanostructured $Co(PO_3)_2$ Anode. *Adv. Funct. Mater.* **2013,** *23*, 227-233.
53. Deng, X.; Öztürk, S.; Weidenthaler, C.; Tüysüz, H. Iron-Induced Activation of Ordered Mesoporous Nickel Cobalt Oxide Electrocatalyst for the Oxygen Evolution Reaction. *ACS Appl. Mater. Interfaces* **2017,** *9*, 21225-21233.
54. Ullman, A. M.; Nocera, D. G. Mechanism of Cobalt Self-Exchange Electron Transfer. *J. Am. Chem. Soc.* **2013,** *135*, 15053-15061.
55. Friebel, D.; Bajdich, M.; Yeo, B. S.; Louie, M. W.; Miller, D. J.; Sanchez Casalongue, H.; Mbuga, F.; Weng, T.-C.; Nordlund, D.; Sokaras, D.; Alonso-Mori, R.; Bell, A. T.; Nilsson, A. On the Chemical State of Co Oxide Electrocatalysts during Alkaline Water Splitting. *Phys. Chem. Chem. Phys.* **2013,** *15*, 17460-17467.
56. Bajdich, M.; García-Mota, M.; Vojvodic, A.; Nørskov, J. K.; Bell, A. T. Theoretical Investigation of the Activity of Cobalt Oxides for the Electrochemical Oxidation of Water. *J. Am. Chem. Soc.* **2013,** *135*, 13521-13530.

TABLE OF CONTENT